ISSN 2706-655X Vol.4, Issue 7: 15-20, DOI: 10.25236/IJFET.2022.040704

Numerical analysis and control of nonlinear traveling wave in cylindrical tube based on neo-Hookean material

Baonan Yang[a], Jindong Liu[b], Bing Yang[c]

School of Computer Science, Xijing University, Xi'an, 710123, P.R. China
[a]yangbaonan@foxmail.com, [b]amosliu@yeah.net, [c]934032350@qq.com

Abstract: *In this paper, the nonlinear wave of a cylindrical tube composed of neo-Hookean material is analyzed. Firstly, the homoclinic orbit of the system not affected by external disturbance is analyzed and calculated by numerical method, then the chaos of the system containing disturbance is analyzed by bifurcation diagram and Lyapunov exponent spectrum, and finally the system is controlled by synchronous coupling control.*

Keywords: *neo-Hookean material, Numerical method, Chaos, Synchronous coupling control*

1. Introduction

As a hyperelastic material, neo-Hookean material has been widely studied [1,2]. The cylindrical tube based on neo-Hookean material has always been the hotspot and focus of neo-Hookean material research. Andrey Melnikov and ray W. Ogden [3] analyzed the bifurcation of a pressurized electroelastic cylindrical tube with closed ends and flexible electrodes on the curved boundary; Luis dorfmann and ray W. Ogden [4] studied the axisymmetric vibration and axisymmetric wave propagation in a cylindrical gent electroelastic model tube; Ran Wang et al. [5] studied the nonlinear wave propagation in a cylindrical tube composed of neo-Hookean materials and gave the ordinary differential equation. In this paper, unbounded nonlinear traveling wave analysis is carried out based on the ordinary differential equation given by ran Wang et al. Based on the nonlinear wave of a cylindrical tube made of neo-Hookean material, when its compressibility is not considered, the system is represented as follows

$$\begin{cases} \dot{x} = y \\ \dot{y} = ax - cx^3 - ky + Fcos\omega t \end{cases} \tag{1}$$

Where a and c are the ratio of anisotropy, shear modulus, material density and wave velocity, $-ky + Fcos\omega t$ is the external disturbance term.

2. Dynamic analysis of undisturbed system

When the system (1) does not contain a disturbance term, it become

$$\begin{cases} \dot{x} = y \\ \dot{y} = ax - cx^3 \end{cases} \tag{2}$$

The analysis shows that the system has three equilibrium points, respectively $(-\sqrt{\frac{a}{c}}, 0)$, $(0,0)$, $(\sqrt{\frac{a}{c}}, 0)$. Where $(0,0)$ is the saddle point, $(\pm\sqrt{\frac{a}{c}}, 0)$ is the center point.

2.1. Homoclinic orbit

According to system (2), its Hamiltonian is $H(x,y) = \frac{1}{2}y^2 + \frac{c}{4}x^4 - \frac{a}{2}x^2$. When $H = 0$, there are two homoclinic orbits connecting saddle points. The expression of homoclinic orbit is solved below

ISSN 2706-655X Vol.4, Issue 7: 15-20, DOI: 10.25236/IJFET.2022.040704

$$\begin{cases} \dot{x} = y \\ \frac{1}{2}y^2 + \frac{c}{4}x^4 - \frac{a}{2}x^2 = 0 \end{cases} \tag{3}$$

Here $y^2 = ax^2 - \frac{c}{2}x^4$, $y = \pm x\sqrt{a - \frac{c}{2}x^2}$, namely $\frac{\mathrm{d}x}{\mathrm{d}t} = \pm x\sqrt{a - \frac{c}{2}x^2}$, $\frac{\mathrm{d}x}{x\sqrt{a-\frac{c}{2}x^2}} = \pm \mathrm{d}t$. Let $x = \sqrt{\frac{2a}{c}}sin\alpha$, then there $\frac{d\alpha}{\sqrt{a}sin\alpha} = \pm \mathrm{d}t$, simultaneous integration of both sides

$$\frac{1}{\sqrt{a}}ln(csc\alpha - cot\alpha) = \pm t + C \tag{4}$$

When $y = 0$ and $t = 0$, from $H = 0$, we can know that $C = 0$, we got $\mathrm{csc}\alpha - cot\alpha = e^{\pm\sqrt{a}t}$, and because $x = \sqrt{\frac{2a}{c}}sin\alpha$, so we know

$$x = \pm\sqrt{\frac{2a}{c}}sech(\sqrt{a}t) \tag{5}$$

The derivative of x can be obtained $y = \mp a\sqrt{\frac{2}{c}}sech(\sqrt{a}t)tanh(\sqrt{a}t)$. Therefore, the two homoclinic orbits corresponding to the system are $z^0(t) = (x_0(t), y_0(t))$

$$\begin{cases} x_0(t) = \pm\sqrt{\frac{2a}{c}}sech(\sqrt{a}t) \\ y_0(t) = \mp a\sqrt{\frac{2}{c}}sech(\sqrt{a}t)\,tanh(\sqrt{a}t) \end{cases} \tag{6}$$

So homoclinic orbit T_1 expression is

$$\begin{cases} x_0(t) = \sqrt{\frac{2a}{c}}sech(\sqrt{a}t) \\ y_0(t) = -a\sqrt{\frac{2}{c}}sech(\sqrt{a}t)\,tanh(\sqrt{a}t) \end{cases} \tag{7}$$

Homoclinic orbit T_2 expression is

$$\begin{cases} x_0(t) = -\sqrt{\frac{2a}{c}}sech(\sqrt{a}t) \\ y_0(t) = a\sqrt{\frac{2}{c}}sech(\sqrt{a}t)\,tanh(\sqrt{a}t) \end{cases} \tag{8}$$

2.2. Numerical analysis of homoclinic orbit

Previous studies often used ode45 algorithm to analyze the homoclinic orbit of the system, without considering the dissipation of the system in the case of long-time numerical integration. In this paper, the homoclinic orbit of the system is numerically analyzed for a long time by using Euler algorithm and symplectic Euler algorithm.

The iterative format of Euler algorithm of system (2) is

$$\begin{cases} x_{n+1} = x_n + hy_n \\ y_{n+1} = y_n + h(ax_n - cx_n^3) \end{cases} \tag{9}$$

The iterative format of the symplectic Euler algorithm of system (2) is

ISSN 2706-655X Vol.4, Issue 7: 15-20, DOI: 10.25236/IJFET.2022.040704

$$\begin{cases} x_{n+1} = x_n + hy_n \\ y_{n+1} = y_n + h(ax_{n+1} - cx_{n+1}^3) \end{cases} \tag{10}$$

Taking homoclinic orbit T_1 as an example, the iteration step length $h = 0.01$, the number of iterations $i = 5000$, $a = \frac{16}{5}$ and $c = \frac{32}{5}$, knowable time domain $t \in [0,50s]$, the phase diagram and sequence diagram are as follows

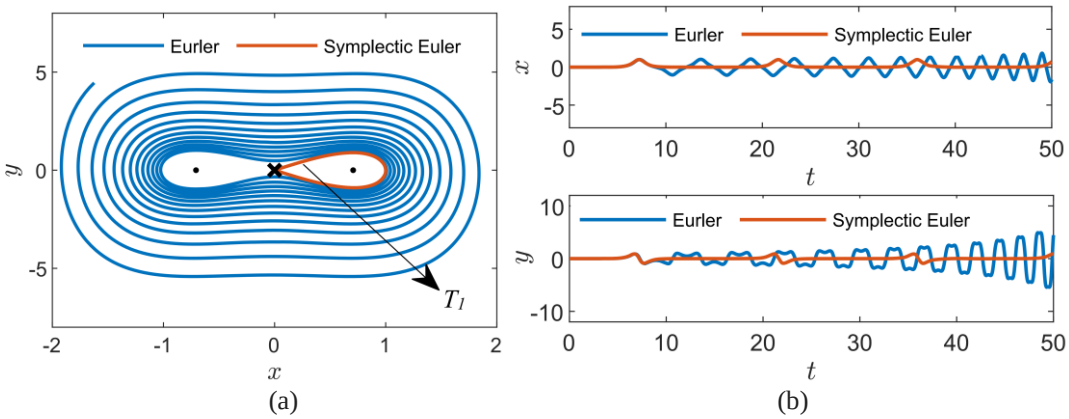

Figure 1: (a) homoclinic orbit T_1. (b) time series.

It can be found from the figure above that in the case of long-time numerical integration, the symplectic Euler algorithm can maintain the structure of the system better than the Euler method, while the Euler method has dissipation.

3. Dynamic analysis of disturbed system

When the system contains disturbance term, it is system (1)

$$\begin{cases} \dot{x} = y \\ \dot{y} = ax - cx^3 - ky + Fcos\omega t \end{cases}$$

System (1) presents different dynamic behaviors under different parameters. Take $a = \frac{16}{5}$, $c = \frac{32}{5}$, $k = 0.5$, $\omega = 1$, F is a variable. It can be seen that the bifurcation diagram and Lyapunov exponent diagram are as follows

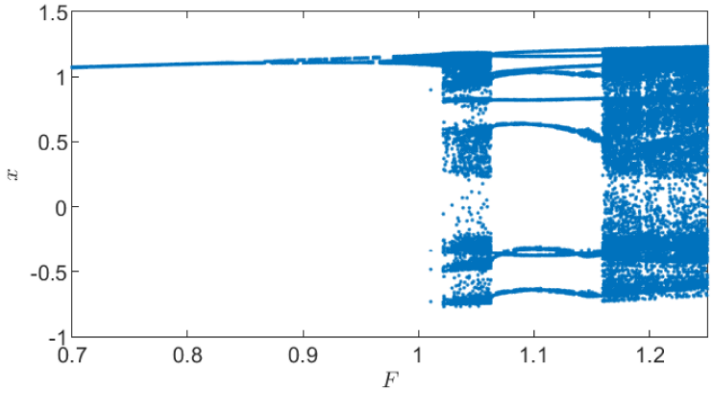

Figure 2: bifurcation diagram.

When the bifurcation diagram is one or several straight lines, it is a periodic state; when the bifurcation diagram is chaotic, it is a chaotic state.

ISSN 2706-655X Vol.4, Issue 7: 15-20, DOI: 10.25236/IJFET.2022.040704

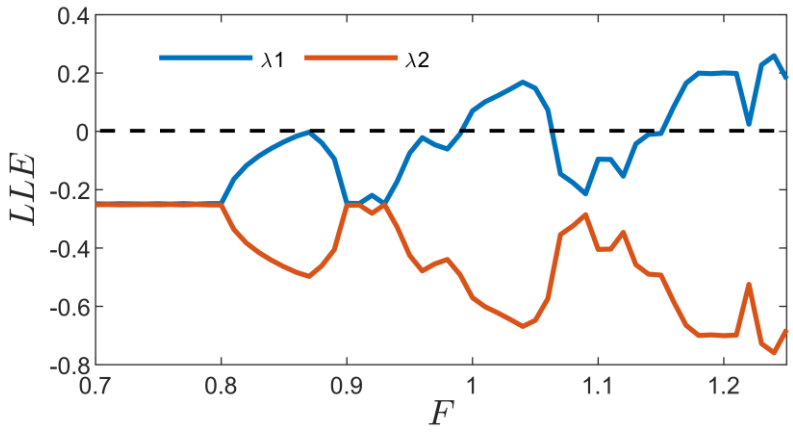

Figure 3: Lyapunov exponent diagram

When the maximum Lyapunov exponent is less than 0, the system is in periodic state, and when it is greater than 0, the system is in chaotic state.

In order to verify the bifurcation diagram and Lyapunov exponent diagram, take $F = 0.75$, the phase diagram, Poincare section and sequence diagram of system (1) are as follows

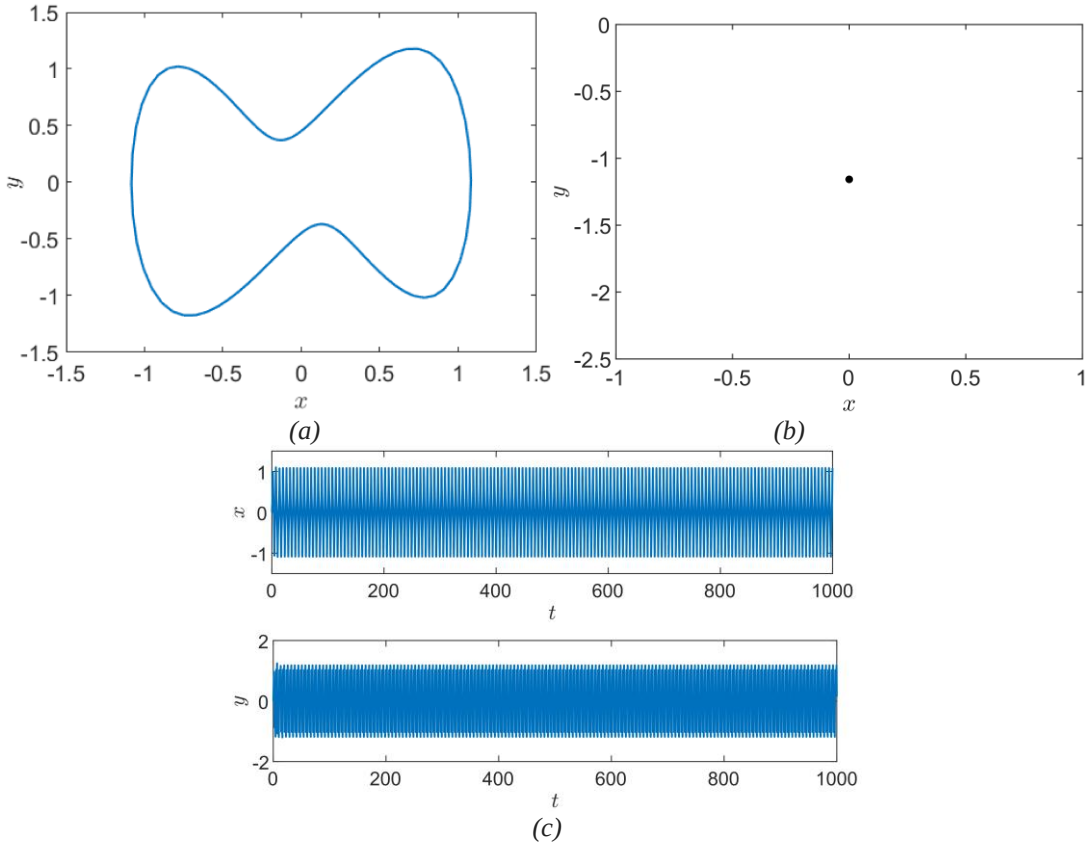

Figure 4: (a) phase diagram. (b) Poincare section and (c) time series.

It can be seen that the system(1) is in periodic state at this time.

Take $F = 1.2$, the phase diagram, Poincare section and sequence diagram of system (1) are as follows

ISSN 2706-655X Vol.4, Issue 7: 15-20, DOI: 10.25236/IJFET.2022.040704

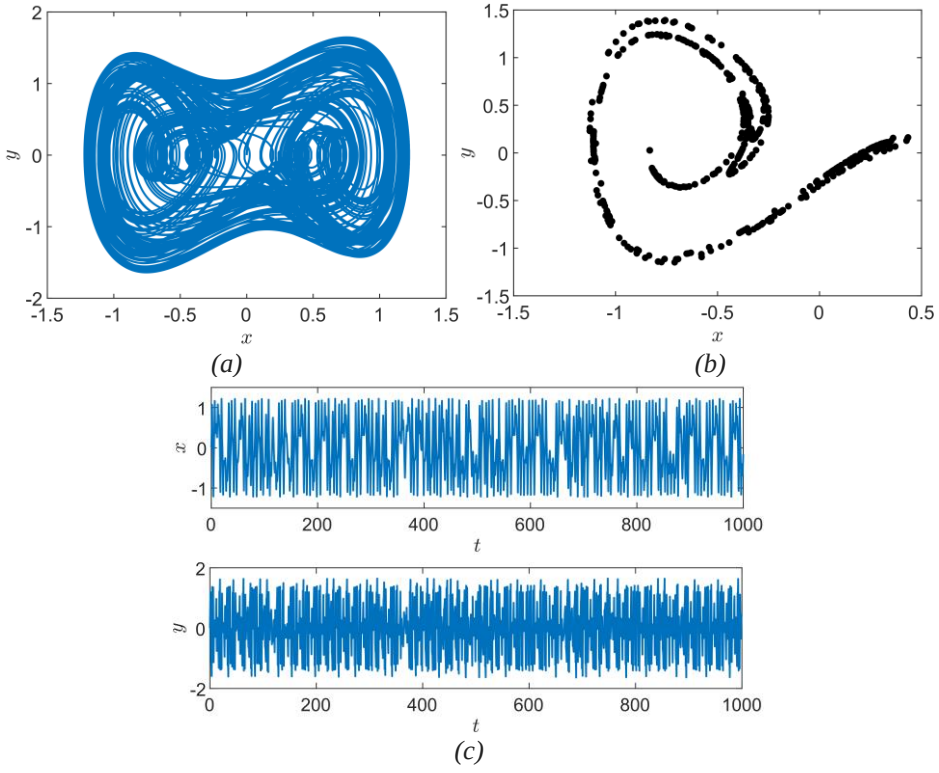

Figure 5: (a) phase diagram. (b) Poincare section and (c) time series.

It can be seen that the system(1) is in a chaotic state at this time.

Fig. 4 and Fig. 5 correspond to the bifurcation diagram and Lyapunov indicator diagram to prove the characteristics of the system(1).

4. Synchronous control of system

When chaos occurs in the system, the structure will often be broken, broken or even damaged, because it is particularly important to design the controller to make the system tend to a stable state. In this paper, the coupling synchronization is used to control the system, and the driving system is as follows

$$\begin{cases} \dot{x} = y \\ \dot{y} = ax - cx^3 - ky + F cos\omega t \end{cases} \tag{11}$$

The response system is designed as follows

$$\begin{cases} \dot{x}_1 = y + k_1(x - x_1) \\ \dot{y}_1 = ax - cx^3 - ky + F cos\omega t + k_2(y - y_1) \end{cases} \tag{12}$$

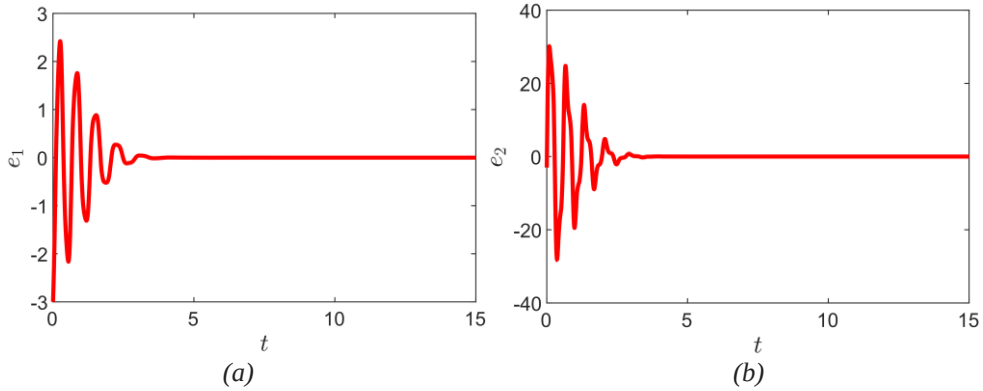

Figure 6: (a) synchronization error $\boldsymbol{e_1}$*. (b) synchronization error* $\boldsymbol{e_2}$*.*

Where, $e_1 = x_1 - x$, and $e_2 = y_1 - y$ is the error between the driving system and the response

ISSN 2706-655X Vol.4, Issue 7: 15-20, DOI: 10.25236/IJFET.2022.040704

system, k_1 and k_2 is the coupling coefficient.

Take $k_1 = 4$ and $k_2 = 2$, the simulation step is 0.01 and the simulation time is 15s. The error diagram is in Figure 6.

From the above simulation results, it can be seen that the system error converges to 0 and the system reaches stability.

5. Conclusion

In this paper, an unbounded nonlinear traveling wave in cylindrical tube based on Neo Hookean material is studied. Firstly, for the system without disturbance term, the homoclinic orbit analysis is carried out by using Euler algorithm and symplectic Euler algorithm. It is found that symplectic Euler algorithm can better maintain the system structure compared with Euler algorithm in the case of long-time numerical integration; Secondly, the system with disturbance term is analyzed by bifurcation diagram and Lyapunov exponent spectrum, its periodic state and chaotic state are found, and the characteristics of the system are verified; Finally, a coupled synchronization controller is designed to control chaos.

References

[1] Guo Z, Caner F, Peng X, et al. On constitutive modelling of porous neo-Hookean composites[J]. Journal of the Mechanics and Physics of Solids, 2008, 56(6): 2338-2357.
[2] Anssari-Benam A, Bucchi A. A generalised neo-Hookean strain energy function for application to the finite deformation of elastomers[J]. International Journal of Non-Linear Mechanics, 2021, 128: 103626.
[3] Melnikov A, Ogden R W. Bifurcation of finitely deformed thick-walled electroelastic cylindrical tubes subject to a radial electric field[J]. Zeitschrift für angewandte Mathematik und Physik, 2018, 69(3): 1-27.
[4] Dorfmann L, Ogden R W. Waves and vibrations in a finitely deformed electroelastic circular cylindrical tube[J]. Proceedings of the Royal Society A, 2020, 476(2233): 20190701.
[5] Wang R, Zhang W, Zhao Z, et al. Radially and axially symmetric motions of a class of transversely isotropic compressible hyperelastic cylindrical tubes[J]. Nonlinear Dynamics, 2017, 90(4): 2481-2494.